

Phase diagram of ^4He adsorbed on graphitePhilippe Corboz,¹ Massimo Boninsegni,² Lode Pollet,¹ and Matthias Troyer¹¹*Institut für Theoretische Physik, ETH Zürich, CH-8093 Zürich, Switzerland*²*Department of Physics, University of Alberta, Edmonton, Alberta, Canada T6G 2J1*

(Received 11 November 2008; published 12 December 2008)

We present results of a theoretical study of ^4He films adsorbed on graphite based on the continuous space worm algorithm. In the first layer, we find a domain-wall phase and a (7/16) registered structure between the commensurate (1/3) and the incommensurate solid phases. For the second layer, we find only superfluid and incommensurate solid phases. The commensurate phase found in a previous simulation work is only observed if first-layer particles are kept fixed; it disappears upon explicitly including their zero-point fluctuations. No evidence of any “supersolid” phase is found.

DOI: 10.1103/PhysRevB.78.245414

PACS number(s): 67.25.dp, 02.70.Ss, 05.30.Jp, 67.80.bd

I. INTRODUCTION

Adsorption of helium on a graphite substrate is still the subject of many experimental and theoretical studies. Although this subject is almost 4 decades old, it has lately been enjoying a resurgence of interest in connection with the study of a possible supersolid phase of matter.

Due to the strong attraction to graphite, helium forms up to seven distinct layers above the substrate,^{1,2} with each layer being a realization of a quasi-two-dimensional system. Several types of phases result from the interplay between the interaction among helium atoms and their interaction with the substrate, including fluid, commensurate (C), and incommensurate (IC) solid phases. Crowell and Reppy³ raised the possibility of a supersolid phase in the second layer from the anomalous behavior of the period shift in torsional oscillator experiments. Supersolids exhibit simultaneously crystalline order and frictionless flow in a single homogeneous phase and have attracted increasing interest since the observation of nonclassical moment of inertia in solid ^4He by Kim and Chan.⁴ It has been proposed, based on a number of fundamental arguments, that a commensurate perfect single crystal of ^4He ought not be supersolid,⁵ a prediction supported by a number of computer simulations.^{6,7} However, a supersolid phase exists for bosonic models on a triangular lattice,⁸ and one may thus speculate about the possibility of supersolids on substrates.⁹

For the first adsorbed helium layer, there exist preferred adsorption sites located above the centers of the hexagons formed by the carbon atoms on the graphite surface. A commensurate phase at filling 1/3, as well as an incommensurate solid phase, is clearly observed in neutron-diffraction experiments,^{10–12} heat-capacity measurements,^{13–15} and in numerical simulations.¹⁶ The identification of the phases occurring between the two solids is still uncertain.¹⁷ Several types of domain-wall (DW) phases have been predicted^{1,18} but none have been unambiguously observed.

The second layer is known to exhibit a gas, a superfluid, and an incommensurate solid phase, as shown by heat-capacity measurements^{15,19} and neutron-diffraction experiments.^{10–12} At intermediate density between these two phases, Greywall and Busch^{1,15} conjectured a commensurate solid with a $\sqrt{7} \times \sqrt{7}$ partial registry with respect to the first

layer based on their heat-capacity measurements. At the same filling, a commensurate solid phase was observed in path-integral Monte Carlo (PIMC) simulations;²⁰ in that study, however, for computational convenience first-layer particles were treated as classical, i.e., held fixed in space at their $T=0$ equilibrium position. Because of the relative weakness of the adsorption potential experienced by second-layer atoms, it is plausible that the explicit inclusion of zero-point motion of first-layer particles, possibly leading to a further weakening of the attraction, may qualitatively alter the picture. Moreover, no prediction has yet been made theoretically regarding the existence of a possible supersolid phase in the second layer.

In this paper, we study the low-temperature phase diagram of the first and second layers of ^4He on graphite by means of state-of-the-art computer simulations in which quantum zero-point motion of helium atoms in both the first and second layers is fully included. Our computed phase diagram is summarized in Fig. 1. In the first layer we find a striped phase, a hexagonal domain-wall phase, and a hexagonal commensurate structure (at filling 7/16) between the two crystals. In the second layer, we do not observe a commensurate solid phase,²¹ in contrast to the predictions by Greywall and Busch.^{1,15} Rather, as coverage is increased the system goes through coexistence of liquid and gas phases, a (superfluid) liquid and an incommensurate crystal.

We show that the commensurate phase observed in Ref. 20 is merely a consequence of the neglect of zero-point motion of first-layer ^4He atoms and that such a phase disappears if this approximation is removed, i.e., if zero-point motion of first-layer particles is included in the simulation. In *no* case will a supersolid phase of ^4He be observed, i.e.,

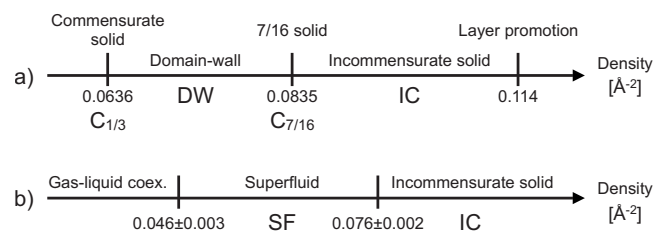


FIG. 1. Schematic phase diagram of the (a) first and (b) second layers as a function of two-dimensional layer density.

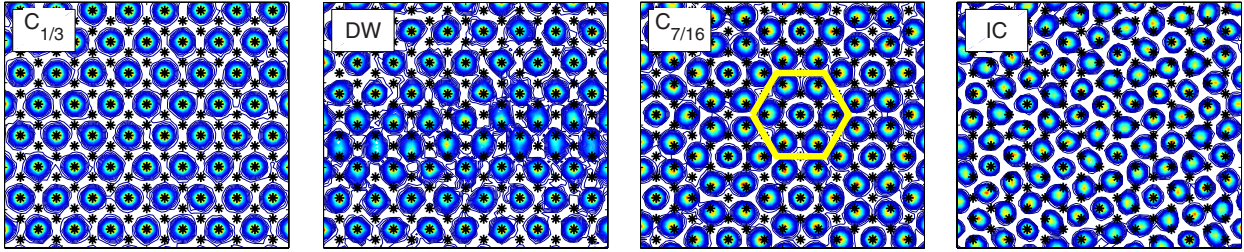


FIG. 2. (Color online) Contour plots of the density distribution of the ^4He atoms in the first layer (x - y plane parallel to the substrate). The black stars mark the minima of the underlying graphite potential (adsorption sites). The distance between two adsorption sites is 2.46 \AA . The snapshots are taken at different densities in the first layer (see Fig. 1). $C_{1/3}$: commensurate $1/3$ solid; DW: domain-wall phase; $C_{7/16}$: commensurate $7/16$ solid; and IC: incommensurate solid.

including when a commensurate second-layer solid phase is “artificially” stabilized by holding first-layer atoms at fixed positions, as done in Ref. 20. Not surprisingly, no supersolid phase occurs in *incommensurate* solid films, in analogy with what is observed in three dimensions.

In Sec. II we briefly illustrate our model and computational methodology. We then describe our results in detail for the first and second layers.

II. METHODOLOGY

Our computer simulations are based on the continuous space worm algorithm.²² This methodology was proven to be remarkably effective in large-scale simulations of Bose systems, owing to its efficiency in sampling multiparticle exchanges, which underlie phenomena such as Bose-Einstein condensation and superfluidity.

The microscopic model utilized here is standard. Specifically, we use the helium Aziz interatomic potential,^{23,24} as well as the anisotropic 6–12 graphite-helium potential of Carlos and Cole²⁵ used in essentially all previous simulation work.²⁶ Such a potential accounts for the corrugation of the graphite substrate, a crucial ingredient needed to describe the variety of registered phases in the first layer. Effects of the corrugation of the graphite substrate become negligible for successive adlayers; for simulations of the second layer we have therefore utilized the laterally averaged version of the Carlos-Cole potential (see also Ref. 20).

Our model is fully three dimensional. We use standard periodic boundary conditions and simulate systems comprising up to 600 particles at temperatures as low as 0.2 K , which is low enough to yield essentially ground-state estimates.

III. RESULTS: FIRST LAYER

In the first layer we confirm the existence of a commensurate $C_{1/3}$ solid at coverage $\rho_{1/3}=0.0636 \text{ \AA}^{-2}$ (Fig. 2). At higher coverage, the film enters a DW phase with stripes of the $C_{1/3}$ solid separated by (superheavy) domain walls.¹⁷

At even higher coverage, we observe a change from striped to hexagonal network of (heavy) domain walls. The possibility of a transition between these two domain-wall types was already raised by Greywall.¹ This network becomes denser with increasing coverage, ending with a com-

mensurate solid ($C_{7/16}$) for $\rho_{7/16}=0.0835 \text{ \AA}^{-2}$, where $7/16$ of the adsorption sites are occupied. This structure is also found in diffraction experiments of D_2 on graphite²⁷ but had not yet been predicted for helium. Greywall¹ proposed a particular commensurate structure around a coverage 0.820 \AA^{-2} , which differs only by 1.8% from $\rho_{7/16}$. Thus, the signal observed in his heat-capacity measurements may stem from the $C_{7/16}$ solid. For densities above $\rho_{7/16}$ we find an incommensurate solid, in agreement with experiments and previous calculations.¹⁶

Next, we determine the layer promotion density ρ_1^{lp} , at which the second layer starts to become populated. At equilibrium, the chemical potentials of the first and the second layers are equal, i.e., $\mu_1(\rho_1, \rho_2)=\mu_2(\rho_1, \rho_2)$, where ρ_1 and ρ_2 are the densities in the first and second layers, respectively. Layer promotion occurs at specific value of the chemical potential μ^{lp} at which the second-layer density ρ_2 jumps from zero to a finite value ρ_2^{min} . Thus, we can find ρ_1^{lp} by solving the equation

$$\mu^{\text{lp}} = \mu_1(\rho_1^{\text{lp}}, 0) = \mu_2(\rho_1^{\text{lp}}, \rho_2^{\text{min}}). \quad (1)$$

In order to determine $\mu_1(\rho_1)$, we performed simulations with a fixed number of particles and with the first layer initialized as a triangular solid. Density scans are obtained by varying the area of the simulation cell. It is

$$\mu_1(\rho_1) = e(\rho_1) + \rho_1 \frac{de}{d\rho_1}, \quad (2)$$

with $e=E/N$ as the energy per particle, where we estimate the derivative from a polynomial fit of degree 4 to $e(\rho)$ as shown in Fig. 3. We determine the chemical potential of the second layer at the minimum coverage ρ_2^{min} by taking the thermalized first-layer simulations and switch to a grand canonical simulation, where we gradually increase μ until the second layer becomes populated. We find $\mu_2 = -29.6 \pm 0.3 \text{ K}$ (essentially independent of ρ_1). The solution of Eq. (1) for ρ_1^{lp} is given by the intersection of the two chemical-potential curves in the right panel of Fig. 3. Comparing results from different simulations (30 and 56 particles), we find $\rho_1^{\text{lp}} = 0.1140 \pm 0.0003 \text{ \AA}^{-2}$.

This value is in agreement with previous simulation results of Whitlock *et al.*,²⁶ who used an effective potential for second-layer particles. It is also compatible with

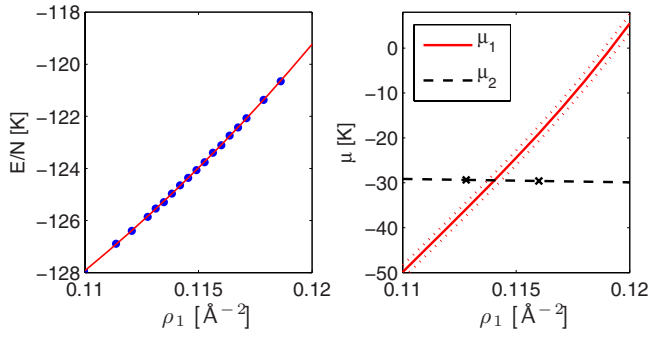


FIG. 3. (Color online) Left plot: energy per particle versus coverage of simulations with a constant number of particles (56) and varying volume. The red line is a polynomial fit of degree 4. Right plot: the red curve corresponds to the chemical potential in the first layer with an error bar given by the red dotted lines. The black dashed line indicates the chemical potential at which the second layer becomes populated. The error bars are smaller than the symbol sizes. The intersection yields the layer promotion density $\rho_1^{\text{lp}} = 0.1140 \pm 0.0003 \text{ \AA}^{-2}$.

neutron-diffraction experiments and heat-capacity measurements,^{10,11,13,19} where values in the range $0.112\text{--}0.115 \text{ \AA}^{-2}$ were found.

Greywall and Busch¹⁵ determined a value of 0.12 \AA^{-2} from heat-capacity measurements, which is higher than our result. However, in Ref. 1 Greywall pointed out that there is an ambiguity in his coverage scale by several percent. Thus, our layer promotion density is consistent with their value, taking their uncertainty into account. We have tested the sensitivity of our result upon deepening the attractive well of ^4He -graphite potential by 10%; we find $\rho_1^{\text{lp}} = 0.1165 \pm 0.0005 \text{ \AA}^{-2}$ in this case, still lower than that of Greywall and Busch.¹⁵ In fact, the value of density corresponding to first-layer promotion proposed by Greywall and Busch¹⁵ is only observed by making the potential more attractive by over 20%, a correction which seems unlikely, as we discuss below.

IV. RESULTS: SECOND LAYER

We now discuss the physics of the second adsorbed helium layer. Adsorption of successive layers causes a compression of the first adlayer experimentally estimated between 4% (Ref. 11) and 6%.¹⁵ In this work, we performed simulations for the second layer based on different first-layer densities, ranging from 0.1164 to 0.1270 \AA^{-2} , with the latter being the value proposed by Greywall and Busch,^{1,15} and assumed by Pierce and Manousakis^{20,28} in their PIMC simulations.

On varying the density of the first layer in the above range, the physics of the second layer does not change qualitatively; typical results are shown in Fig. 4. Specifically, we *only* find a superfluid and an incommensurate solid phase separated by a first-order phase transition. We do *not* observe a commensurate solid phase sandwiched between the liquid and the incommensurate crystal, in contrast to the prediction of Greywall and Busch.¹⁵

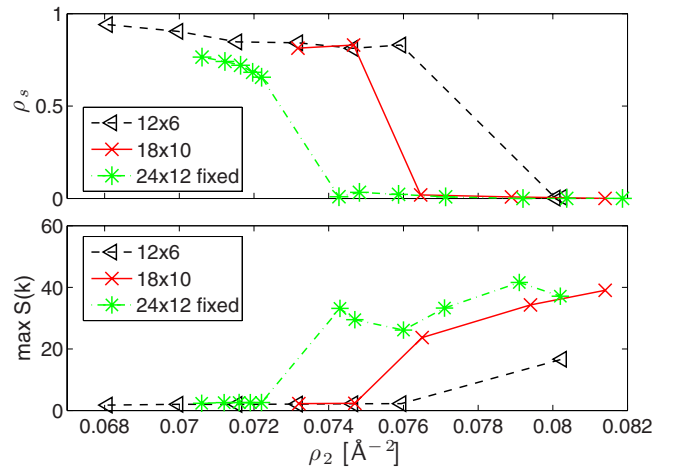


FIG. 4. (Color online) Upper panel: ^4He superfluid density. Lower panel: peak values of the static structure factor. Data shown are for the second layer at temperature $T=0.5 \text{ K}$. The system sizes are given as multiples of the first-layer unit cell. The first-layer density is $\rho_1 = 0.1202 \text{ \AA}^{-2}$ (0.1270 \AA^{-2}) in simulations with active (fixed, stars) first-layer particles. Statistical errors are of the order of symbol sizes.

The two-dimensional (2D) equilibrium density of the liquid second layer, in the $T \rightarrow 0$ limit, is estimated at $0.046(3) \text{ \AA}^{-2}$, essentially independent of first-layer density. In order to give an idea of the weakness of the adsorption potential seen by second-layer atoms, one may note that the above equilibrium density is indistinguishable from that of purely two-dimensional ^4He (Ref. 29) and significantly lower than that of a ^4He monolayer on a lithium substrate (the weakest known substrate wetted by ^4He).³⁰ This liquid film turns superfluid at low T , as we established by direct computation of the superfluid density ρ_s , based on the well-known winding number estimator.³¹

Assuming a first-layer density of 0.1202 \AA^{-2} (corresponding to a 5% compression), the onset value of coverage for the occurrence of superfluidity is therefore $0.166(3) \text{ \AA}^{-2}$ (Fig. 1). As shown in Fig. 4 (crosses and triangles), the superfluid density vanishes at a 2D density of $0.076 \pm 0.002 \text{ \AA}^{-2}$, corresponding to a coverage of $0.196 \pm 0.002 \text{ \AA}^{-2}$, at which the incommensurate crystal phase appears. These coverages are altogether consistent with existing measurements once experimental uncertainties are properly taken into account.³

In the heat-capacity measurements of Greywall and Busch,¹⁵ a peak appears around a coverage of 0.197 \AA^{-2} , which they associate with a commensurate structure. They assumed a compressed first-layer density of 0.1270 \AA^{-2} . From the ratio of first- and second-layer densities ($\approx 4/7$), Greywall¹ conjectured a $\sqrt{7} \times \sqrt{7}$ registered structure with one quarter of the second-layer atoms located directly above the first-layer atoms; this has also been proposed for the second layer of ^3He on graphite.³² To our knowledge, however, no direct experimental evidence for the commensurate phase has been reported. One possible scenario is that the observed peak in the heat capacity is a signature of the incommensurate phase, which in our simulations appears at the same coverage.

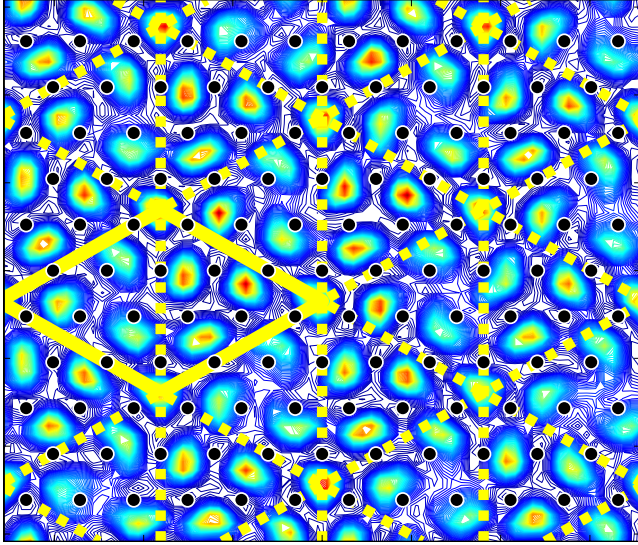


FIG. 5. (Color online) Snapshot of the commensurate 7/12 solid in the second layer, which only appears in simulations with fixed first-layer particles with a first-layer density of $\rho_1=0.1270 \text{ \AA}^{-2}$. The black dots mark the positions of the first-layer particles (repulsion sites). Second-layer particles found at the intersections of the thick dotted (yellow) lines are located above the middle of three neighboring first-layer particles. The (yellow) thick line marks a unit cell of the 7/12 solid. The ^4He superfluid density in this phase is zero.

In the PIMC simulations of Ref. 20, the 4/7 commensurate structure was observed (with a different positioning of the second-layer atoms with respect to the first layer), assuming the first-layer density proposed by Greywall and Busch.¹⁵ However, as mentioned above, in these simulations first-layer particles were held *fixed*, i.e., their zero-point motion was neglected. On performing the same simulation, we also observe a commensurate structure (Fig. 4), albeit at a slightly different filling (7/12). It consists of a triangular lattice rotated by an angle of 10.89° with respect to the first layer, as shown in the snapshot in Fig. 5. The difference in density compared to the 4/7 filling is only $\approx 2\%$. The superfluid density of such a commensurate phase is *zero*, i.e., no evidence of a possible supersolid phase is found (see Fig. 4).

As shown in Figs. 4 and 6, no commensurate phase arises if first-layer particles are simulated *explicitly* even if the (relatively high) first-layer density of 0.127 \AA^{-2} utilized in Ref. 20 is assumed. This is because due to zero-point motion, first-layer atoms occupy a larger region of space than predicted classically. Thus, second-layer atoms are slightly pushed away from the first layer (see Fig. 7), which reduces the substrate attraction by $\sim 3 \text{ K}$, enough to destabilize the commensurate phase (see also Ref. 33). It should also be noted that even with fixed first-layer particles, no commensurate phase is observed if a first-layer density lower than 0.127 \AA^{-2} is assumed (Fig. 6).

Regardless of whether first-layer particles are held fixed or not, at sufficiently high coverage an *incommensurate* crystalline phase forms (see Fig. 4). Such a phase is also not superfluid, consistent with what is now regarded as a fairly general theoretical statement.⁵

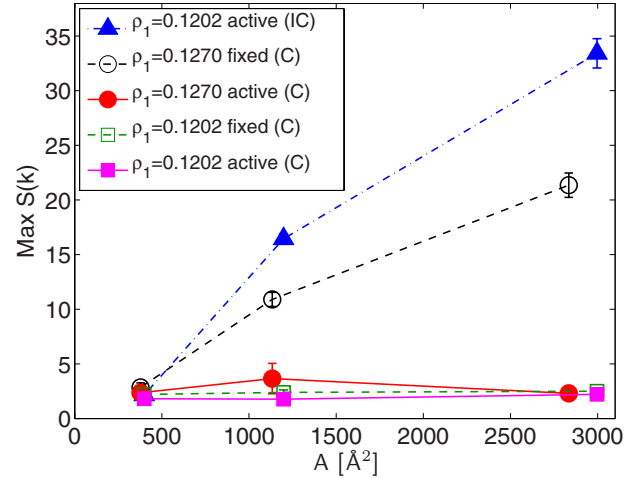


FIG. 6. (Color online) Scaling of the structure factor peak with system size A (area) at temperature $T=0.5 \text{ K}$. Results obtained from active/fixed first-layer particles for two different first-layer densities ρ_1 are shown. The incommensurate solid (triangles, IC) is always stable and independent of the first-layer density. The second-layer density is $\rho_2=0.080 \text{ \AA}^{-2}$ in this example. For all the other data points the coverage corresponds to one of the commensurate 7/12 solid. Only in the case of fixed first-layer particles and highest first-layer density $\rho_1=0.1270 \text{ \AA}^{-2}$, the commensurate solid is stable in the thermodynamic limit.

Just like for the issue of first-layer promotion, we have explored the possibility that a revision of the helium-graphite potential might indeed stabilize the commensurate second-layer phase which we do not observe using the Carlos-Cole potential as originally proposed in Ref. 25. Simulations with a 10% deeper substrate potential also failed to yield a stable commensurate solid, except at the very largest first-layer density $\rho_1=0.1270 \text{ \AA}^{-2}$ (which is however not compatible with our value for ρ_1^{fp}), where the 7/12 commensurate solid becomes stable. We discuss below whether a quantitative revision of the potential seems justified in light of known experimental facts.

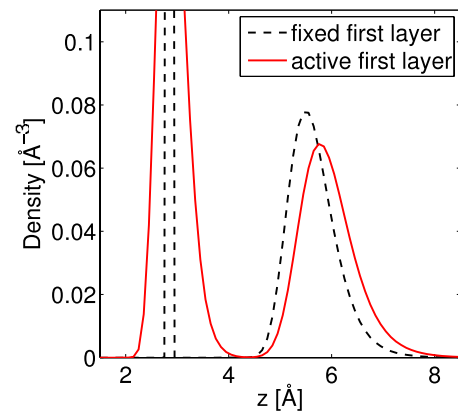


FIG. 7. (Color online) Comparison between the density profiles of a system with fixed (dashed line) and active (full line) first-layer particles at a total coverage of $\rho=0.2117 \text{ \AA}^{-2}$. In the latter case the second layer is displaced by $\approx 0.3 \text{ \AA}$ away from the substrate due to the zero-point motion of the first-layer particles.

V. CONCLUSIONS

We have carried out a thorough computational study of the first and second layers of ^4He adsorbed on a graphite substrate based on the most realistic interaction potentials currently available, which are utilized in all previous simulation work. For the first layer, our results largely confirm those of others and are consistent with experimental results.

Conversely, our simulations show no commensurate second-layer phase, in contrast to the interpretation of heat-capacity measurements by Greywall and Busch.^{1,15} Rather, we only observed a liquid layer (superfluid at low temperature), which crystallizes at high density to form an incommensurate solid. The physical behavior of the second layer is thus very close to that of a purely two-dimensional system, also looking at the narrow spread of the ^4He density in the perpendicular direction and at the nonexistent overlap of first- and second-layer particles shown in Fig. 7, pointing to the absence of interlayer quantum exchanges. It is also worth pointing out the similarity between the physics of the second layer of ^4He on graphite and that of a monolayer adsorbed on a lithium substrate.^{30,34}

Our prediction of no commensurate phase is at variance with previous numerical work by Pierce and Manousakis,²⁰ who observed it instead in their PIMC simulations. It needs to be stressed, however, that there is no significant *numerical* disagreement between our results and those of Ref. 20. Our different conclusion directly stems from the fact that, unlike Pierce and Manousakis,²⁰ we did not keep first-layer particles fixed but rather simulated their zero-point motion explicitly. This fact alone accounts for (most of) the difference between the physical outcomes of the two studies. It is worth noting that the possible importance of the role of quantum fluctuations of inner layer particles had already been suggested by other authors.³³

The absence of a commensurate phase suggests that either the experimental data have to be reinterpreted or the microscopic model adopted so far, chiefly the helium-graphite potential, might have to undergo significant revisions. We have studied this scenario at the same length, in this work, notably by rendering the attractive well of the potential deeper. If the attraction is increased by some 10% (while fully retaining in the simulation the zero-point motion of first-layer ^4He atoms), a commensurate crystalline phase is observed *only* if a density of 0.127 \AA^{-2} is assumed for the first layer, i.e., the value proposed by Greywall and Busch.¹⁵ This value is consistent with the first-layer promotion density computed in this work with such a revised potential (i.e., 10% more attractive), only on assuming a compression of the inner adlayer of some 9% upon adsorption of successive layers. This degree of compression is substantially above that estimated by most experimental studies. In any case, a revision of such a quantitative degree of the helium-graphite potential proposed by Carlos and Cole seems doubtful, in view of the good agreement with experimental data presented in Ref. 25.

Finally, no finite superfluid signal is seen in any of the crystalline phases observed, either the incommensurate or the commensurate (the latter, as explained above, merely occurs as the result of treating inner layer particles as fixed in the simulation). Thus, we conclude that this system is not a realistic candidate for the observation of a supersolid phase.

ACKNOWLEDGMENTS

We acknowledge inspiring discussions with N. Prokof'ev, J. Nyéki, and J. Saunders. Simulations were performed on the Brutus Beowulf cluster at ETH Zurich. This work was supported by the Natural Science and Engineering Research Council of Canada under Grant No. G12120893 and the Swiss National Science Foundation.

¹D. S. Greywall, Phys. Rev. B **47**, 309 (1993).

²G. Zimmerli, G. Mistura, and M. H. W. Chan, Phys. Rev. Lett. **68**, 60 (1992).

³P. A. Crowell and J. D. Reppy, Phys. Rev. Lett. **70**, 3291 (1993); Phys. Rev. B **53**, 2701 (1996).

⁴E. Kim and M. H. W. Chan, Nature (London) **427**, 225 (2004); Science **305**, 1941 (2004).

⁵N. Prokof'ev and B. Svistunov, Phys. Rev. Lett. **94**, 155302 (2005).

⁶M. Boninsegni, N. Prokof'ev, and B. Svistunov, Phys. Rev. Lett. **96**, 105301 (2006).

⁷B. K. Clark and D. M. Ceperley, Phys. Rev. Lett. **96**, 105302 (2006).

⁸M. Boninsegni and N. Prokof'ev, Phys. Rev. Lett. **95**, 237204 (2005); D. Heidarian and K. Damle, *ibid.* **95**, 127206 (2005); S. Wessel and M. Troyer, *ibid.* **95**, 127205 (2005); R. G. Melko, A. Paramekanti, A. A. Burkov, A. Vishwanath, D. N. Sheng, and L. Balents, *ibid.* **95**, 127207 (2005).

⁹J. Saunders (private communication). It should be noted that there is a qualitative difference between a system in which crystalline order arises from the spontaneous breaking of translational symmetry, and one in which it is imposed by an external potential, as would be the case for an adsorbed film registered with the underlying substrate.

¹⁰K. Carneiro, L. Passell, W. Thomlinson, and H. Taub, Phys. Rev. B **24**, 1170 (1981).

¹¹H. J. Lauter, H. P. Schildberg, H. Godfrin, H. Wiechert, and R. Haensel, Can. J. Phys. **65**, 1435 (1987).

¹²H. J. Lauter, H. Godfrin, V. L. P. Frank, and P. Leiderer, in *Phase Transitions in Surface Films 2*, edited by E. Taub, G. Torzo, H. J. Lauter, and S. C. Fain (Plenum, New York, 1991).

¹³M. Bretz, J. G. Dash, D. C. Hickernell, E. O. McLean, and O. E. Vilches, Phys. Rev. A **8**, 1589 (1973).

¹⁴S. V. Hering, S. W. Van Sciver, and O. E. Vilches, J. Low Temp. Phys. **25**, 793 (1976); R. E. Ecke and J. G. Dash, Phys. Rev. B **28**, 3738 (1983).

¹⁵D. S. Greywall and P. A. Busch, Phys. Rev. Lett. **67**, 3535 (1991).

- ¹⁶M. E. Pierce and E. Manousakis, Phys. Rev. B **62**, 5228 (2000).
- ¹⁷L. W. Bruch, M. W. Cole, and E. Zaremba, *Physical Adsorption* (Dover, New York, 1997).
- ¹⁸T. Halpin-Healy and M. Kardar, Phys. Rev. B **34**, 318 (1986).
- ¹⁹S. E. Polanco and M. Bretz, Phys. Rev. B **17**, 151 (1978).
- ²⁰M. Pierce and E. Manousakis, Phys. Rev. Lett. **81**, 156 (1998); Phys. Rev. B **59**, 3802 (1999).
- ²¹In the present system a *commensurate* second layer implies commensurability with respect to the first layer and not with respect to the graphite substrate. The corrugation of the graphite-helium potential is negligible in the second layer.
- ²²M. Boninsegni, Nikolay Prokof'ev, and B. Svistunov, Phys. Rev. Lett. **96**, 070601 (2006); M. Boninsegni, N. V. Prokof'ev, and B. V. Svistunov, Phys. Rev. E **74**, 036701 (2006).
- ²³R. A. Aziz, V. P. S. Nain, J. S. Carley, W. L. Taylor, and G. T. McConville, J. Chem. Phys. **70**, 4330 (1979).
- ²⁴In Ref. 20 a slightly different version of the Aziz potential was used, which does not deviate significantly from the one used here.
- ²⁵W. E. Carlos and M. C. Cole, Surf. Sci. **91**, 339 (1979).
- ²⁶P. A. Whitlock, G. V. Chester, and B. Krishnamachari, Phys. Rev. B **58**, 8704 (1998).
- ²⁷H. Freimuth, H. Wiechert, H. P. Schildberg, and H. J. Lauter, Phys. Rev. B **42**, 587 (1990).
- ²⁸In a computer simulation making use of a finite cell, only one first-layer coverage will be compatible with triangular crystal-line arrangement. As a result, the relative densities of first and second layers do *not* change in the course of the simulation.
- ²⁹M.-C. Gordillo and D. M. Ceperley, Phys. Rev. B **58**, 6447 (1998).
- ³⁰M. Boninsegni and L. Szybisz, Phys. Rev. B **70**, 024512 (2004).
- ³¹D. M. Ceperley, Rev. Mod. Phys. **67**, 279 (1995).
- ³²V. Elser, Phys. Rev. Lett. **62**, 2405 (1989).
- ³³P. A. Whitlock, G. V. Chester, and B. Krishnamachari, Comput. Phys. Commun. **121-122**, 460 (1999).
- ³⁴M. Boninsegni, M. W. Cole, and F. Toigo, Phys. Rev. Lett. **83**, 2002 (1999).